The polymerization of actin: Thermodynamics near the polymerization line

Priya S. Niranjan and Peter B. Yim
Department of Chemistry and Biochemistry, The University of Maryland College Park, College Park, Maryland 20742

Jeffrey G. Forbes
Proteomics and Nanotechnology Section, Laboratory of Muscle Biology, NIAMS, NIH, DHHS, Bethesda, Maryland 20892

Sandra C. Greer[a)]
Department of Chemistry and Biochemistry, and Department of Chemical Engineering, The University of Maryland College Park, College Park, Maryland 20742

Jacek Dudowicz and Karl F. Freed
The James Franck Institute and the Department of Chemistry, The University of Chicago, Chicago, Illinois 60637

Jack F. Douglas
Polymers Division, National Institute of Standards and Technology, Gaithersburg, Maryland 20899

(Received 13 January 2003; accepted 23 May 2003)

Studies of the dependence of actin polymerization on thermodynamic parameters are important for understanding processes in living systems, where actin polymerization and depolymerization are crucial to cell structure and movement. We report measurements of the extent of polymerization, Φ, of rabbit muscle actin as a function of temperature $[T=(0-35)\,^{\circ}\mathrm{C}]$, initial G-actin concentration $[[G_0]=(1-3)\ \mathrm{mg/ml}]$, and initiating salt concentration $[[\mathrm{KCl}]=(5-15)\ \mathrm{mmol/l}$ with bound $\mathrm{Ca}^{2+}]$, in H_2O and D_2O buffers and in the presence of adenosine triphosphate (ATP). A preliminary account of the data and analysis for H_2O buffers has appeared previously [P. S. Niranjan, J. G. Forbes, S. C. Greer, J. Dudowicz, K. F. Freed, and J. F. Douglas, J. Chem. Phys. **114**, 10573 (2001)]. We describe the details of the studies for H_2O buffers, together with new data and analysis for D_2O buffers. The measurements show a maximum in $\Phi(T)$ for H_2O buffers and D_2O buffers. For H_2O buffers, T_p decreases as either $[G_0]$ or [KCl] increases. For D_2O buffers, T_p decreases as [KCl] increases, but T_p is not monotonic in $[G_0]$. The measurements are interpreted in terms of a Flory–Huggins-type lattice model that includes the essential steps: monomer activation, dimerization of activated species, and propagation of trimers to higher order polymers. The competition between monomer activation and chain propagation leads to the observed nonmonotonic variation of $\Phi(T)$. The actin polymerization in D_2O buffer differs considerably from that in the H_2O buffer and underscores the significant deuterium effect on hydrophobic interactions and hydrogen bonding in the polymerization process. © *2003 American Institute of Physics.* [DOI: 10.1063/1.1592499]

I. INTRODUCTION

The manifold of biological functions for the protein actin arises from the control of the polymerization of monomeric globular G-actin into polymeric filaments of F-actin.[1,2] The concentration of actin in the cytoplasm of nonmuscle cells is about (1–5) mg/ml, with up to half of the actin in the unpolymerized state.[3] Numerous studies focus on how regulatory proteins (e.g., capping, cross-linking, polymerizing, and depolymerizing, nucleating, etc.) control actin polymerization under physiological conditions.[4,5] Although many regulatory proteins have been identified, there is limited understanding of how they act concertedly on actin to produce complex nonequilibrium processes, such as cell protrusion and movement.[6] Recent studies of the role of actin polymerization in cell migration have suggested that changes in thermodynamic variables, such as temperature and concentrations, could play a role in regulating actin polymerization.[7,8] This hypothesis is motivated by the supposition that polymerization occurs in an environment in which there are local spatial gradients and temporal oscillations in the concentrations of actin monomer, salts, and regulatory proteins.[7,9] The polymerization transition of actin is sensitive to these thermodynamic variables, and it is important to quantify how changes in these solution variables influence actin polymerization.

Thus, we focus here on the influence of temperature, salt concentration, and total G-actin concentration in the regulation of actin polymerization. The reversible polymerization of actin has most often been considered at a fixed temperature, as the concentration of initial G-actin is increased to a ''critical concentration'' in the presence of activating salts that catalyze the reaction by a mechanism not yet fully

a)Author to whom correspondence should be addressed. Electronic mail: sg28@umail.umd.edu

understood.[10] If, instead, we fix the initial actin and salt concentrations and vary temperature,[11] then the polymerization beyond the dimer stage commences at a ''floor temperature,''[12] or ''polymerization temperature,'' T_p. The reversible polymerization of actin can be viewed as a rounded phase transition, like similar polymerizations in organic and inorganic systems and as found in systems with applied fields and finite size constraints.[13–16]

A key variable in treating reversible polymerizations from a phase transition perspective is the extent of polymerization, Φ, which is the fraction of the initial monomer that has been incorporated into polymers at equilibrium at each temperature, T.[17] The extent of polymerization can be viewed loosely as a kind of ''order parameter,''[18] and is important in the theories of reversible polymerizations.[13,16] In this paper, T_p is designated as the temperature corresponding to the inflection point in $\Phi(T)$. As will be shown elsewhere,[19] the theory of equilibrium polymerization described below predicts that the temperature of the inflection point can be distinct from the temperature at which the heat capacity has a maximum, so that the definition of T_p is not unique. However, we expect that these two temperatures will exhibit similar trends.

We present a study of Φ for rabbit muscle actin as a function of the initial concentration $[G_0]$ of G-actin, of the concentration [KCl] of initiating salt, and of temperature, T, in H_2O and D_2O buffers, prepared with one Ca^{2+} counterion bound to each monomer and in solution with adenosine triphosphate (ATP). A preliminary report on the data for H_2O buffers has appeared.[20] We describe here the details of the studies for H_2O buffers, together with new data and analysis for D_2O buffers. While studies of the critical concentrations of actin at fixed T (25 °C) have been published (see review in Ivkov *et al.*[11]), those experiments use rather high fixed salt concentrations ($\approx$100 mM) (Ref. 21) and rather low initial actin $[G_0]$ concentrations ($<$0.3 mg/ml). Our experiments, in contrast, span $[G_0]$ values of (1–3) mg/ml (23–69 μM), the range found in living cells.[3,22] The concentrations [KCl] in our experiments (5 mM, 9 mM, and 15 mM) are lower than in previous work[10,23,24] and are chosen so that the polymerization temperatures are in an experimentally accessible range of (0–35) °C. These salt concentrations are lower than the average salt concentrations in living cells,[25] but cell contents are not homogeneous and lower salt concentrations may exist in different cellular regions.

At every fixed $[G_0]$ and [KCl], we observe an increase of Φ as the temperature reaches T_p, followed by an maximum in Φ above T_p. This maximum was not anticipated, since measurements of Φ for polymerizations in organic systems vary monotonically, exhibiting a plateau in the polymerized region.[17] This feature has not been noted before for actin, although there is evidence in neutron scattering studies.[11] We suggest that it has not been noted because T was not often been varied in earlier measurements.

The polymerization of actin is described with a statistical mechanical model of the Flory–Huggins-type.[26] The polymerization mechanism includes an activation of the monomer, a dimerization of two activated species, the formation of a trimer as the smallest propagating oligomer, and the propagation of trimers into higher order polymers occurring above a polymerization temperature, T_p. Several different polymerization mechanisms produce identical calculated actin equilibrium mass distributions, but the essential steps of the reaction process seem to be robust—an activation of monomer, reversible dimerization of activated monomer, and propagation to form long chains. With three adjustable enthalpy parameters and three adjustable entropy parameters, the model provides a very satisfactory description of the experimental data.

We also present studies of the thermodynamics of actin polymerization in a deuterated aqueous buffer. In living cells, the aqueous environment is certainly not deuterated. However, the shift from H_2O to D_2O is accompanied by changes in hydrogen bond strength and in hydrophobic interactions, and the analysis of these phenomena provides clues concerning the complex interactions between water and actin. The deuteration effect on the hydrogen bonding in the water and between the water and the protein can alter the basic interactions controlling the polymer association. Thus, deuteration is not a small perturbation of the solution characteristics, as the actin data demonstrate. In addition, D_2O is used in a variety of studies on proteins (e.g., neutron scattering, nuclear magnetic resonance, kinetics), so it is important to understand the behavior of proteins in deuterium oxide.

II. THEORY: LATTICE MODEL OF ACTIN POLYMERIZATION

Initially, the system is composed of n_1^0 monomers of G-actin, n_{KCl} molecules of salt (KCl), and n_s molecules of H_2O. The first stage of actin polymerization is believed to involve activation and dimerization of initiated actin monomers,[4,27] followed by the growth of F-actin filaments.[1,28] The activated monomers and dimers react to form trimers (the ''nucleus''), and the trimers associate with monomers to yield higher mass polymers.[10] We consider actin solutions where these processes occur under equilibrium conditions. Several mechanisms are found to produce the same equilibrium relative molecular mass distribution upon redefinition of free energy parameters. The theory is illustrated first with one model before specifying some essentially equivalent alternatives. The first model is based on the minimal reaction scheme,

$$A_1 \rightleftarrows A_1^* \quad \text{(monomer activation)}, \tag{1}$$

$$A_1^* + A_1^* \rightleftarrows A_2 \quad \text{(dimerization)}, \tag{2}$$

$$A_2 + A_1^* \rightleftarrows A_3 \quad \text{(trimer formation)}, \tag{3}$$

$$A_i + A_1 \rightleftarrows A_{i+1}, \quad i = 3,4,...,\infty \quad \text{(propagation)}, \tag{4}$$

where A_1 designates a G-actin monomer, an asterisk denotes an activated species, and the subscript i indicates the degree of polymerization. Activation is thought to be triggered by a conformational change of the actin monomer through ion binding.[29] A similar hierarchy of reactions for actin polymerization is employed by Cooper *et al.* in kinetic studies of

actin polymerization,[29] and the evidence for this reaction scheme is discussed elsewhere.[1,4,27,28,30]

For simplicity, the free energies associated with the propagation reactions (3) and (4) are taken as identical, so the distribution of actin species at a given T is governed by three equilibrium constants or, equivalently, by three free energies: the free energy of activation $\Delta f_{\rm actv}=\Delta h_{\rm actv}-T\Delta s_{\rm actv}$, the free energy of dimerization $\Delta f_{\rm dim}=\Delta h_{\rm dim}-T\Delta s_{\rm dim}$, and the free energy of propagation $\Delta f_{\rm prop}=\Delta h_{\rm prop}-T\Delta s_{\rm prop}$. At equilibrium, the system contains n_1 unreacted monomers A_1, n_1^* activated monomers A_1^*, $\{n_i\}$ polymers $\{A_i\}$ $(i=2,3,...,\infty)$, and n_s solvent molecules. The conservation of actin mass constraint requires that n_1^* and $\{n_i\}$ are related to the initial number n_1^0 of G-actin monomers by

$$n_1^0=n_1^*+\sum_{i=1}^{\infty} in_i. \tag{5}$$

The equilibrium system is described by an incompressible Flory–Huggins (FH) type lattice model[15,16] in which each A_i species occupies i lattice sites and each solvent molecule covers a single lattice site. Thus, the total number N_l of lattice sites is written in terms of the numbers for the individual species as

$$N_l=n_s+n_1^*+\sum_{i=1}^{\infty} in_i=n_s+n_1^0, \tag{6}$$

where we have ignored the volume occupied by the salt molecules and by the other components of the buffer solution. In addition, despite the huge size disparity between water molecules and G-actin monomers, the treatment allowing an actin monomer to occupy a much larger number of lattice sites than individual solvent molecules can be transcribed into the final equations (presented below in terms of volume fractions) through a redefinition of the apparent reaction entropies (see below). A prior communication[20] presents a derivation of the equilibrium fraction Φ of G-actin converted to actin polymers, based solely on the application of the law of mass action to Eqs. (1)–(4). However, here we provide a more general derivation that involves computing the free energy of the system, an approach that enables the determination of diverse equilibrium thermodynamic properties of actin solutions.

The total Helmholtz free energy F for the system in the FH model for stiff associating polymers is given by[16,26]

$$\frac{F}{N_l k_B T}=f_{\rm salt}+\phi_s\ln\phi_s+\phi_1^*\ln\phi_1^*+\sum_{i=1}^{\infty}\frac{\phi_i}{i}\ln\phi_i+\phi_s\phi_1^*\chi+\phi_s\chi\sum_{i=1}^{\infty}\phi_i+\phi_1^* f_1^*+\sum_{i=2}^{\infty}\phi_i f_i, \tag{7}$$

where $\phi_s=n_s/N_l$, $\phi_1^*=n_1^*/N_l$, and $\{\phi_i=in_i/N_l\}$ denote the volume fractions for the solvent, the activated actin monomers, and actin polymers, respectively, χ designates the monomer–solvent interaction parameter, f_i is the dimensionless specific free energy of an i-mer, f_1^* is the analogous free energy for an activated monomer, and k_B is the Boltzmann constant. The quantity $f_{\rm salt}$ contains the translational and electrostatic free energies of the added salt and is taken as independent of the concentrations of actin species. Contributions to the electrostatic energy that depend on the actin concentration $\{\phi_i\}$ are subsumed in f_i, which implies that the free energy parameters of reactions (1)–(4) that are included in f_i may depend on salt and G-actin concentrations. The specific free energies f_1^* and $\{f_i\}$ are quoted below in Eqs. (14)–(16), while the quantities f_1 and f_s (corresponding to an unactivated actin monomer and the solvent, respectively) are taken as vanishing identically (defining the zero of energy) and are, therefore, absent in Eq. (7). The mass conservation constraint from Eq. (5) can be conveniently reexpressed in terms of volume fractions as

$$\phi_1^0=\phi_1^*+\sum_{i=1}^{\infty}\phi_i, \tag{8}$$

where $\phi_1^0=n_1^0/N_l$.

The condition of chemical equilibrium imposes the following relations between the chemical potentials μ_1, μ_1^*, and μ_i, where the subscripts 1 and i represent, respectively, the monomer A_1 and i-mer A_i and where the asterisk refers to the activated species,

$$\mu_1=\mu_1^*, \tag{9}$$

and

$$\mu_i=i\mu_1, \quad i=2,3,...,\infty. \tag{10}$$

On the other hand, the chemical potentials μ_i can be calculated directly from the free energy of Eq. (7) as,

$$\frac{1}{k_B T}(\mu_i-i\mu_s)=\left.\frac{\partial(F/k_B T)}{\partial n_i}\right|_{T,N_l,n_{j\neq i}}. \tag{11}$$

The exchange chemical potential $\mu_i^{\rm ex}=\mu_i-i\mu_s$ (with μ_s the solvent chemical potential) emerges from Eq. (7) as a consequence of the assumed incompressibility of the system. After some algebra, the equilibrium conditions in Eqs. (9) and (10) reduce to

$$\ln\left[\frac{\phi_1^*}{\phi_1}\right]=-f_1^*, \tag{12}$$

and

$$\ln\left[\frac{\phi_i}{\phi_1^i}\right]=i-1-if_i, \quad i=2,3,...,\infty. \tag{13}$$

The specific energies f_1^*, f_2, and f_i $(i=3,4,...,\infty)$ are obtained by appending to the expression appropriate to Flory–Huggins theory for semiflexible linear polymers[31] the free energies of the reaction processes from Eqs. (1)–(4). Thus, we have

$$f_1^*=\Delta f_{\rm actv}/k_B T, \tag{14}$$

$$f_2=(1/2)\ln[2/(2z)]+(1/2)+(1/2)(2\Delta f_{\rm actv}+\Delta f_{\rm dim})/k_B T, \tag{15}$$

and

$$f_i=\frac{1}{i}\ln\left[\frac{2}{zi}\right]+\frac{i-1}{i}+\frac{3}{i}\frac{\Delta f_{\rm actv}}{k_BT}+\frac{1}{i}\frac{\Delta f_{\rm dim}}{k_BT}+\frac{i-2}{i}\frac{\Delta f_{\rm prop}}{k_BT},\quad i\geqslant 3, \tag{16}$$

where z is the lattice coordination number, while $\Delta f_{\rm actv}$, $\Delta f_{\rm dim}$, and $\Delta f_{\rm prop}$ designate the free energy changes due to the activation, dimerization, and propagation step, respectively. Combining Eqs. (12)–(13) and (14)–(16) leads to the compact expressions for the volume fractions ϕ_1^* and ϕ_i,

$$\phi_1^*=\phi_1\exp(-\Delta f_{\rm actv}/k_BT), \tag{17}$$

$$\phi_2=2\phi_1^2\exp[-(2\Delta f_{\rm actv}+\Delta f_{\rm dim})/k_BT)], \tag{18}$$

and

$$\phi_i=iCA^i,\quad (i=3,4,...,\infty), \tag{19}$$

with the quantity A given by

$$A=\phi_1\exp(-\Delta f_{\rm prop}/k_BT) \tag{20}$$

and with the prefactor C as

$$C=(z/2)\exp[-(3\Delta f_{\rm actv}+\Delta f_{\rm dim}-2\Delta f_{\rm prop})/k_BT]. \tag{21}$$

The extent of polymerization, Φ, is the fraction of monomers converted into polymers,

$$\Phi=(\phi_1^0-\phi_1-\phi_1^*)/\phi_1^0, \tag{22}$$

where $\phi_1^0\equiv[G_0]$ is the initial G-actin volume fraction before polymerization, and ϕ_1 and ϕ_1^* are the equilibrium volume fractions of nonactivated and activated actin monomers, respectively. Conservation of actin mass from Eq. (8) can be conveniently rewritten as

$$\phi_1^0=\phi_1+\phi_1^*+\phi_2+\sum_{i=3}^{\infty}\phi_i. \tag{23}$$

Substituting Eqs. (17)–(21) into Eq. (23) and performing the summation yield,

$$\phi_1^0=\phi_1+\phi_1\exp(-\Delta f_{\rm actv}/k_BT)+2\phi_1^2\exp[-(2\Delta f_{\rm actv}+\Delta f_{\rm dim})/k_BT]+\frac{CA^3}{(1-A)^2}(3-2A), \tag{24}$$

with A and C defined by Eqs. (20) and (21), respectively. Equation (24) is solved numerically for the equilibrium G-actin monomer volume fraction ϕ_1 in terms the dimensionless free energies $\Delta f_{\rm actv}/k_BT$, $\Delta f_{\rm dim}/k_BT$, and $\Delta f_{\rm prop}/k_BT$. Invoking the standard relation $\Delta f=\Delta h-T\Delta s$ enables the computation of $\Phi(T)$ as a function of T for a given set of enthalpies and entropies for activation, dimerization, and propagation. These six adjustable parameters of the theory are taken as temperature independent quantities to simplify the analysis of experimental data, but, in general, they may vary with temperature.

Alternative mechanisms: Several alternative mechanisms lead to the same final computed equilibrium properties after a redefinition of various free energies, and now we present two illustrative examples. Consider, for instance, a mechanism in which the monomer A_1 in step (4) is replaced by the activated monomer A_1^*. The distribution of actin clusters is still governed by the scaling in Eq. (19), with the quantities A and C renormalized to equal,

$$A'=\phi_1\exp(-(\Delta f'_{\rm prop}+\Delta f'_{\rm actv})/k_BT), \tag{25}$$

$$C'=(z/2)\exp[-(\Delta f'_{\rm dim}-2\Delta f'_{\rm prop})/k_BT], \tag{26}$$

where the new free energy parameters $\Delta f'_{\rm actv}$, $\Delta f'_{\rm dim}$, and $\Delta f'_{\rm prop}$ are related to those present in Eqs. (20) and (21) by

$$\Delta f'_{\rm actv}=\Delta f_{\rm actv}, \tag{27}$$

$$\Delta f'_{\rm dim}=\Delta f_{\rm dim}+\Delta f_{\rm actv}, \tag{28}$$

$$\Delta f'_{\rm prop}=\Delta f_{\rm prop}-\Delta f_{\rm actv}. \tag{29}$$

Within this redefinition procedure, only the concentrations of actin dimers differ slightly because the distribution $\phi_i=iC'(A')^i$ applies for $i\geqslant 3$ in Eq. (19). Another possible model, such as one involving the presence of only nonactivated actin monomers in steps (3) and (4) and a single activated actin monomer in step (2) may also be shown as equivalent to those described above after introducing an appropriate renormalization of the free energy parameters. This equivalence of several models leaves intact the fact that all of the related mechanisms contain three essential steps, activation, reversible dimer formation, and chain propagation.

The theoretical computations given above specify the actin monomer as providing the unit of volume, i.e., of occupying a single lattice site, so, effectively, n water molecules are taken to occupy a single lattice site, where n is the ratio of the actin to water molecule volumes. This specification has also been chosen because the ratio n is not well known. Alternatively, individual water molecules can be assigned to single lattice sites, whereupon the actin monomer must occupy n lattice sites. The free energy expression in Eq. (7) then becomes replaced by

$$\frac{F}{N_lk_BT}=f_{\rm salt}+\phi_s\ln\phi_s+\frac{\phi_1^*}{n}\ln\phi_1^*+\sum_{i=1}^{\infty}\frac{\phi_i}{in}\ln\phi_i+\phi_s\phi_1^*\chi+\phi_s\chi\sum_{i=1}^{\infty}\phi_i+\phi_1^*f_1^*+\sum_{i=2}^{\infty}\phi_if_i, \tag{30}$$

where $\phi_s=n_s/N_l$, $\phi_1^*=nn_1^*/N_l$, and $\{\phi_i\}=inn_i/N_l$ and where

$$f_2=(1/2n)\ln[2/(2zn)]+([2n-1]/2n)+(1/2n)(2\Delta f_{\rm actv}+\Delta f_{\rm dim})/k_BT, \tag{31}$$

and

$$f_i=\frac{1}{in}\ln\left[\frac{2}{zin}\right]+\frac{in-1}{in}+\frac{3}{in}\frac{\Delta f_{\rm actv}}{k_BT}+\frac{1}{in}\frac{\Delta f_{\rm dim}}{k_BT}+\frac{i-2}{in}\frac{\Delta f_{\rm prop}}{k_BT},\quad i\geqslant 3. \tag{32}$$

The final distribution emerges with the identical scaling behavior of Eq. (19), except that A'' and C'' are given by

$$A'' = \phi_1 (1/n) \exp(-\Delta f''_{\text{prop}}/k_B T), \tag{33}$$

$$C'' = (zn/2) \exp[-(3\Delta f_{\text{actv}} + \Delta f''_{\text{dim}} - 2\Delta f''_{\text{prop}})/k_B T]. \tag{34}$$

This equivalence implies that the three ΔH are identical between the two models, but the entropies for two of the reactions are redefined as

$$\Delta S''_{\text{dim}} = \Delta S_{\text{dim}} - k_B \ln n, \tag{35}$$

$$\Delta S''_{\text{prop}} = \Delta S_{\text{prop}} - k_B \ln n. \tag{36}$$

The molecular interpretation of these entropies must thus be considered carefully and critically. Independent experimental determinations of these parameters are desirable, but are a challenge at this time.

III. EXPERIMENTAL METHODS

A. General

Pyrene-labeled actin fluoresces significantly more in the polymerized state than in the unpolymerized state. Thus, the measurement of pyrene fluorescence is the most sensitive and accurate assay for actin polymerization.[32,33] The fluorescence of actin samples with 3% (by mass) pyrene labeling, in buffer with initiating salt, is measured as the temperature is increased. This method differs from earlier approaches, where the temperature is held fixed and salt is added to drive the polymerization: Here the salt is present in the initial sample, and temperature is used to drive the polymerization. After completion of the measurements, each sample is completely polymerized in order to scale the measurements and to convert the fluorescence intensities into extents of polymerization.

The fluorescence labeling procedure rests on the assumption that the pyrene-labeling of the actin does not change its thermodynamic properties. This assumption is supported by (1) the consistency of these measurements of T_p from $\Phi(T)$ on pyrene-labeled actin in H_2O buffers with determinations of T_p on unlabeled actin samples using precision mass densimetry,[34] (2) by the consistency of these Φ measurements of T_p for pyrene-labeled actin in D_2O buffers with determinations of T_p for unlabeled actin samples in D_2O buffers using small angle neutron scattering,[11] and (3) by published tests of this assumption.[33]

B. Actin preparation

1. General

The purification procedure for actin has been described in detail in our previous work.[11,35] All vessels used in the actin purification are of plastic, except for the glass Sephacryl column,[36] since protein adheres to glass and since glass also induces the polymerization of actin.[35] Rabbit muscle acetone powder is prepared from fresh rabbit tissue as described by Pardee and Spudich.[37] The actin is extracted from the acetone powder into buffer A [4 mM *tris*, 0.2 mM Na_2ATP, 0.5 mM 2-mercaptoethanol, 0.2 mM $CaCl_2$, 0.005% NaN_3, in nanopure H_2O] and adjusted with HCl(aq) to a final *p*H of 8.0 at 24 °C. The resulting G-actin solution is polymerized by adding KCl to a final concentration of 50 mM, by increasing the ATP concentration to 1 mM and by adjusting the $MgCl_2$ concentration to 2 mM. The solution is stored at 4 °C as F-actin stock solution at about 3 mg/ml of actin.

The stock solution is diluted to about 0.5 mg/ml actin; more KCl, ATP, and $MgCl_2$ are added to ensure full polymerization, and the solution is ultracentrifuged at 150 000×g to make a pellet of F-actin. The pellet is resuspended in buffer A, and then depolymerized by dialysis in a collodion bag (13 000 molecular mass cut-off, Schleicher and Schuell) against buffer A at 4 °C with rapid stirring, for ≈12 h. The resulting G-actin solution is then centrifuged at 120 000×g for 1.5 h at 4 °C to pellet any remaining F-actin. The supernatant solution of G-actin is further purified by size exclusion chromatography (Sephacryl S-200, Amersham Pharmacia Biotech, Piscataway, NJ), using buffer A. If necessary, the actin solution is concentrated by use of a centricone (Amicon Filtration, Millipore, Bedford, MA; molecular mass cut-off=12 000).[11] The purified G-actin is studied within 48 h.

2. D_2O buffer

For the experiments in the D_2O buffer, the purified protein sample in the H_2O buffer A is dialyzed against a D_2O buffer, using the materials and procedure described by Ivkov *et al.*[11] The final stage of dialysis is against a buffer made from 99.9% by mass deuterated D_2O.

3. Pyrene labeling

The method of Kouyama and Mihashi[38] is used to label the actin. F-actin stock solution is diluted to 1 mg/ml, completely polymerized by adding KCl, ATP, and $MgCl_2$, and then dialyzed against buffer A plus KCl, ATP, and $MgCl_2$ (but with no 2-mercaptoethanol, because 2-mercaptoethanol inhibits the binding of the dye). N-(1-pyrenyl)iodoacetamide (Molecular Probes, Eugene, OR; 4 mM in 33 mass % acetone +67 mass % dioxane) is added to the dialyzed F-actin solution in a 4:1 molar ratio of dye to actin, and allowed to react for 12 h on ice. Dithiothreitol is added to a final concentration of 1 mM to quench the unreacted dye. The sample is then ultracentrifuged at 120 000 × g for 1.5 h at 4 °C. The resulting yellow pellet is homogenized and depolymerized by dialysis against buffer A, as described above. The dialyzed, labeled G-actin is purified on a Sephacryl column as above. The labeled G-actin concentration is calculated by measuring the UV absorbance at 344 nm and by using an extinction coefficient[38] of $2.2\times10^4\ \text{mol}^{-1}\ \text{cm}^{-1}$.

The labeled and purified G-actin is mixed with unlabeled purified G-actin to produce a mixture of 3% by mass labeled actin and 97% by mass unlabeled actin.

4. Actin analysis

G-actin concentrations are determined from the UV absorbance at 290 nm, using an extinction coefficient[39] of $\epsilon_{290} = 0.63\ \text{cm}^3/\text{mg}$ and subtracting the absorbance at 330 nm

to correct for scattering. Actin purity is assessed by sodium dodecyl sulfate-polyacrylamide gel electrophoresis (SDS-PAGE). The actin purity is analyzed before and after each of the experiments described below. All analyses find purity $>95\%$.

5. Final steps

The initiating salt, KCl, is added to the actin in buffer at 0 °C, and the final solution is maintained at 0 °C for 6–8 h before experiments are begun.

C. Measurement of the extent of polymerization

We have established[35] that glass cells influence the polymerization of actin and can even initiate the polymerization of actin, in the absence of any initiating salt. Therefore, the spectrometer cells used in this work are made from ''Spectrosil vitreous silica'' (Starna Cells, Inc.), a synthetic quartz. The optical windows of these cells are of Spectrosil and the other walls of Vitreosil. The cells have been constructed by fusing the walls; no adhesives are present. All cells have interior dimensions of 4 mm×4 mm×45 mm, and nominal volumes of 0.56 ml. The cells are rinsed several times with 10% HCl and then cleaned by sonication in deionized nanopure water. All cells are oven dried at 120 °C before use. Cells filled with nanopure water show no fluorescence at 407 nm.

The fluorescence intensity is measured by an Aminco Bowman Series 2 Luminescence Spectrometer (Thermo Spectronic, Rochester, NY), fitted with a monochromator for the emitted light. The excitation wavelength λ_{ex} is set at 365 nm, resulting in emission wavelengths at $\lambda_{em}=387$ and 407 nm. For each G-actin solution containing KCl, the experiment is started at 0.5 °C, and the temperature is raised in steps of 2 °C to a maximum of (30–48) °C. At each temperature, the fluorescence signal at 407 nm, $I(T)$, is followed as a function of time until it reaches a steady-state, which requires about 25 min.[35,40] Figure 1(a) presents a typical equilibration curve.

After the maximum temperature is reached, the sample is completely polymerized by bringing the concentration of $MgCl_2$ to 15 mM. The fluorescence intensity at 407 nm measured from this fully polymerized sample is denoted as I_F. Typical measurements of I_F are presented in Fig. 1(b) and indicate that I_F does not change appreciably with temperature. For one sample in H_2O buffer and one in D_2O buffer, each with $[G_0]=3$ mg/ml and [KCl]=0.0, the fluorescence intensity at 407 nm is measured as a function of T and is denoted by $I_G(T)$. These data at 3 mg/ml are used to analyze all the samples [see Eq. (37)] by scaling to the appropriate $[G_0]$ (e.g., by multiplying by 2/3 for $[G_0]=2$ mg/ml). Figure 1(b) shows that $I_G(T)$ is small and depends little on temperature. The extent of polymerization as a function of T, $\Phi(T)$, is calculated from the expression,

$$I(T)=\Phi(T)I_F+[1-\Phi(T)]I_G(T)', \tag{37}$$

where $I_G(T)'$ is $I_G(T)$, scaled to the $[G_0]$ of the particular sample.

The temperature is controlled to ±0.1 °C by circulating a mixture of water and ethylene glycol around the sample cell. The temperature is measured with a resolution of ±0.1 °C by a thermocouple placed at the cell.

Experimental uncertainties: The uncertainty of the temperature measurement is ±0.1 °C, which can be taken as three standard deviations. The fluorescence intensity can be measured with an instrumental resolution of four significant figures. The scatter in the data for a given sample is 5%–10%. The reproducibility for separate sample preparations ranges between 10%–20% (see below). We therefore report experimental values for the extent of polymerization to two significant figures, to which we assign a precision of 10% and an uncertainty of 20%.

IV. EXPERIMENTAL RESULTS

A. Extent of polymerization measurements in the H_2O buffer

1. General observations for H_2O buffers

Measurements of $\Phi(T)$ are made in H_2O buffer A at three actin concentrations (1.0 mg/ml, 2.0 mg/ml, and 2.9 mg/ml), and, for each actin concentration, at three KCl concentrations (nominally 5, 9, and 15 mM). Figure 1(c) illustrates the reproducibility of these measurements on two different samples of actin, prepared at two different times from two different protein samples: While there is some difference in $\Phi(T)$ between the two actin samples of Fig. 1, the qualitative behavior is the same, and this level of reproducibility is good (10%–20%), given the inherent variability of protein preparations.

The data for $\Phi(T)$ in the H_2O buffer are displayed in Figs. 2 and 3 and are presented in Table I. Figure 2 shows the data for $[G_0]$ fixed, and three different KCl concentrations, while Fig. 3 depicts $\Phi(T)$ for [KCl] fixed and $[G_0]$ variable. Figures 2 and 3 confirm the expected increase in $\Phi(T)$ as the temperature approaches T_p. We further note that:

(1) The polymerization transition occurs over a broad range of T (10–20 °C). Recall that T_p is operationally defined as the point of inflection of $\Phi(T)$.[16]
(2) Figure 2 indicates that T_p diminishes as [KCl] increases. The exact role of the salt in the polymerization mechanism is not fully understood, but these experiments suggest that the enthalpies and entropies of the chain activation and propagation are modified by the salt. This is not surprising, since the actin monomer is a highly charged polyampholyte and the addition of salt screens the electrostatic interactions of the monomers from one another, modifies the counterion clouds, and may even affect the monomer conformation (see below).
(3) Figure 3 indicates that T_p decreases as $[G_0]$ increases. This behavior is expected for a system for which the enthalpy and entropy changes for the propagation reaction are positive.[41]
(4) $\Phi(T)$ increases to a maximum and then decreases at higher temperature. As first reported in our own brief note,[20] this nonmonotonic variation is not due to the degradation of the protein because, as mentioned above, we analyze the protein by gel electrophoresis before and af-

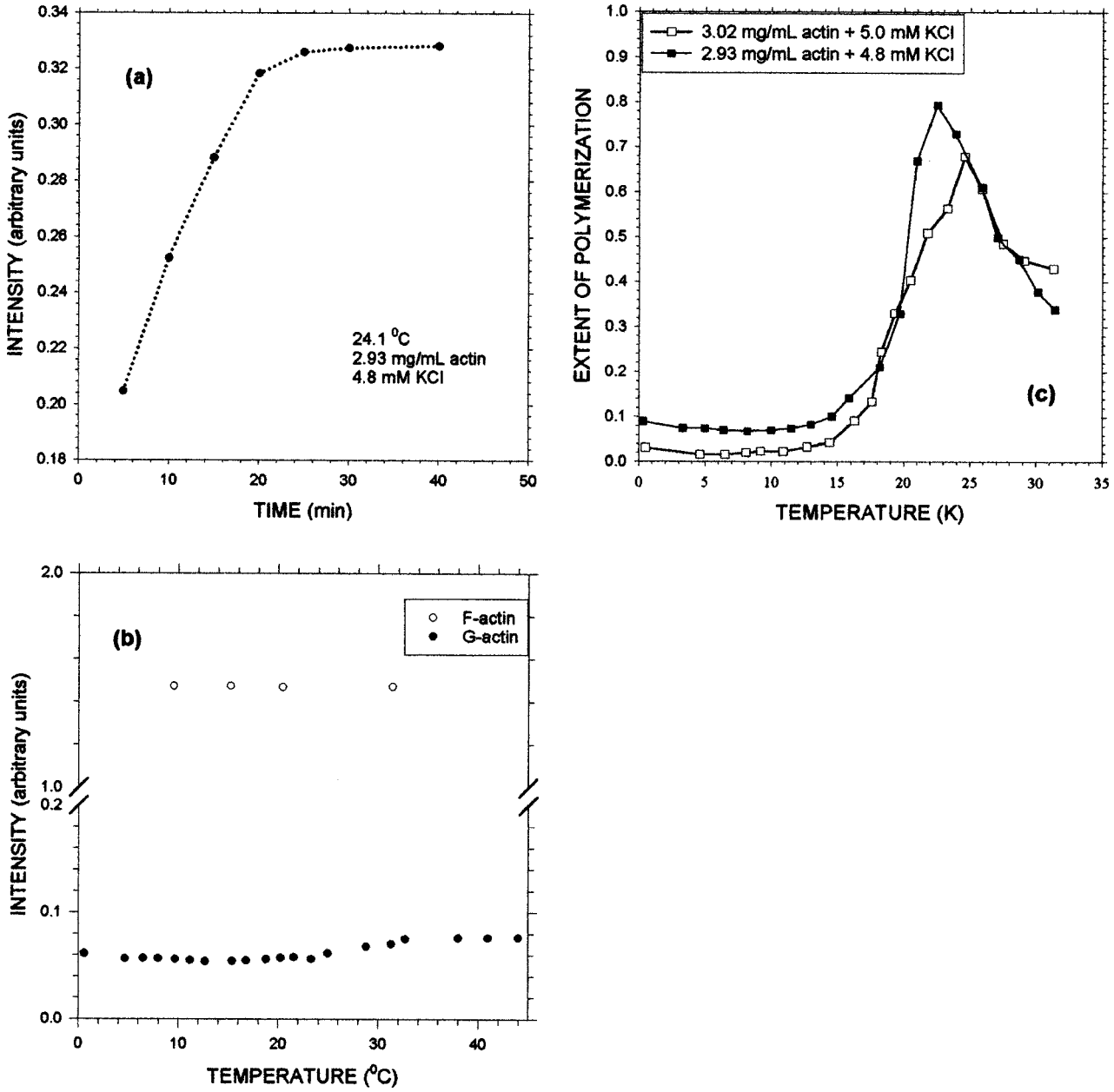

FIG. 1. (a) Fluorescence intensity (in arbitrary units) as a function of time for rabbit muscle action ($[G_0]=2.93$ mg/ml, [KCl]=4.78 mM) in the H_2O buffer. (b) Fluorescence intensity (in arbitrary units) as a function of temperature for (●) unpolymerized G-actin ($[G_0]=3.02$ mg/ml) in the H_2O buffer with no added KCl, and (○) for fully polymerized F-actin ($[G_0]=3.05$ mg/ml) in the H_2O buffer ([KCl]=5.00 mM, $[MgCl_2]=15$ mM). (c) Extent of polymerization Φ as a function of temperature for two actin samples in the H_2O buffer. The samples from two different tissue preparations have nearly the same $[G_0]$ (□ $[G_0]=3.02$ mg/ml and ■ $[G_0]=2.93$ mg/ml) and [KCl] (5 mM), to illustrate the reproducibility of the measurements.

ter each experiment, and see no change. For reversible living polymerizations of synthetic polymers on cooling, $\Phi(T)$ increases to a plateau and does not exhibit a maximum.[16,17] The maximum in $\Phi(T)$ for actin indicates a net depolymerization at higher temperatures, a behavior that is reminiscent of the maximum observed in measurements of the viscosity of polymerizing sulfur[42] and in computer simulations of the extent of polymerization of sulfur.[43] For actin, neutron scattering experiments[11] and mass density measurements[34] also show evidence of such a maximum in $\Phi(T)$.

As explained in our previous Communication, the maximum in $\Phi(T)$ arises from the competition between monomer activation and chain propagation.[20] Figure 4 illustrates this effect explicitly through a comparison of the concentration of activated monomer, $[G^*]$, as a function of T with the concentration of unactivated monomer, $[G]$, and the sum $[G^*]+[G]$. Evidently the increase in $[G^*]$ and the decrease in $[G]$ result in a minimum in $[G^*]+[G]$ that corresponds to the maximum in $\Phi(T)$. Although T_p is monotonic in $[G]$, the decrease of Φ upon heating effectively corresponds to a kind of ''re-entrancy'' of the phase transition.

(5) $\Phi(T)$ is nonzero even well below T_p. The well-known reversible formation of dimers by actin[27,44] is included in

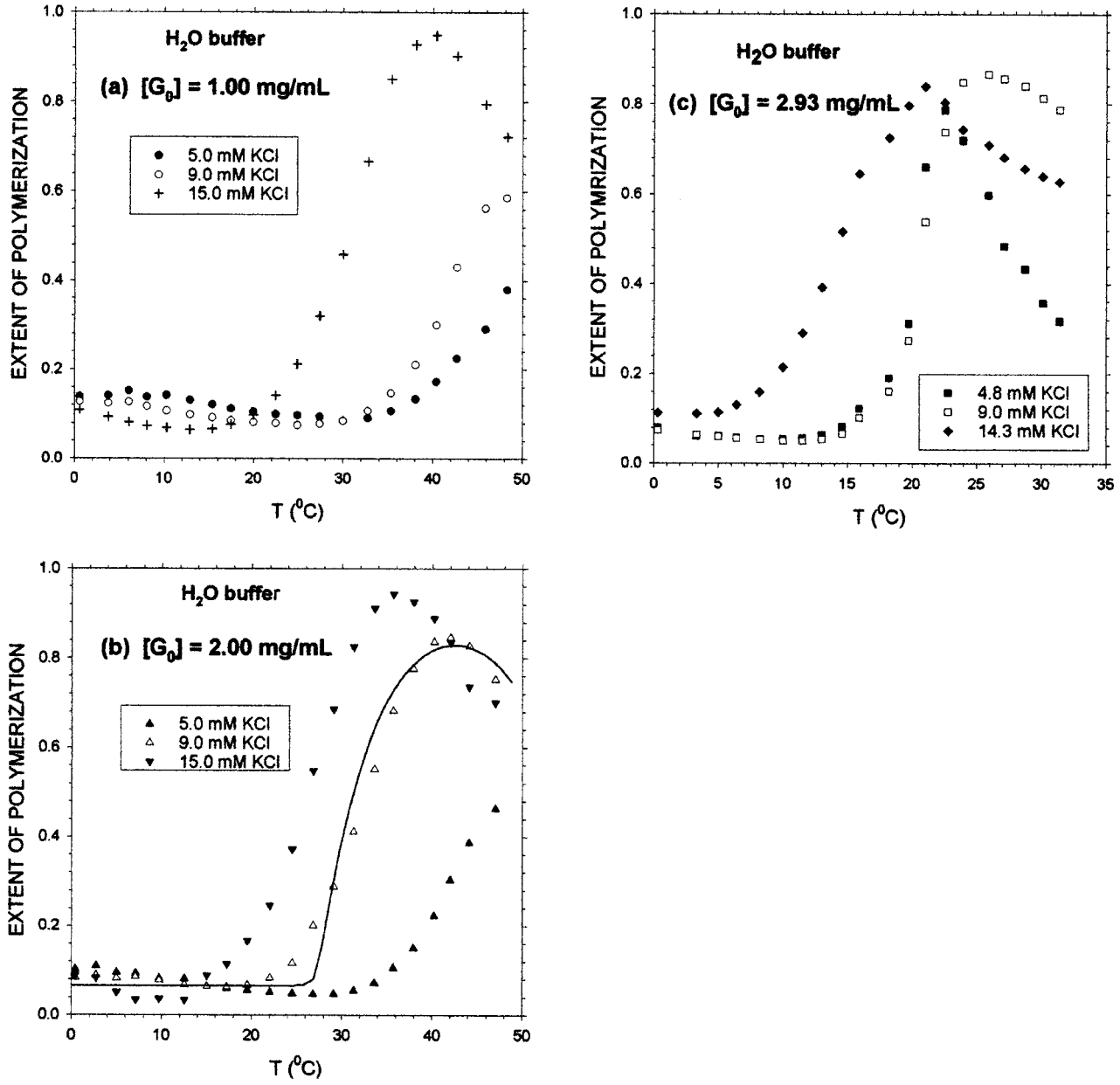

FIG. 2. Extent of polymerization Φ as a function of temperature for rabbit muscle actin in H_2O buffers at fixed initial concentrations of G-actin, $[G_0]$=(a) 1.00 mg/ml, (b) 2.00 mg/ml, and (c) 2.93 mg/ml, for three [KCl] values=5.0 mM, 9.0 mM, and 15.0 mM in each case. The line is the fit of the theory to the data (see text).

the theoretical model and accounts for this low temperature polymerization.[27,45]

(6) The fluorescence intensity (I_F) for a fully polymerized actin sample increases with [KCl]. The increase is largest for the 2.9 mg/ml actin solution where $I_F=0.92$ for [KCl]=4.8 mM, 1.6 for 9.0 mM, and 1.7 for 14.3 mM.[40] Since the change in fluorescence upon polymerization is thought to be due to a change in the G-actin cleft near Cys-374,[46] then our observation suggests that salt is instrumental in that change in conformation.

(7) Because of the coupling between the propagation and the activation, as mentioned in item (4) above and as discussed further below, the Van't Hoff plots that are common in biochemical studies[10,24,47] are not appropriate for polymerizing actin. This issue will be discussed in detail from a theoretical standpoint in a separate paper.[19]

2. Comparision to the theoretical model for H_2O buffers

The results for the H_2O buffer are discussed in our earlier report, which included a table of fitted parameters.[20] Figures 2 and 3 show theoretical fits to experimental data for $\Phi(T)$. The free energy parameters are fitted by applying Eqs. (23) and (24) to each $[KCl]/[G_0]$ data set separately and by visual inspection. A more formal least-squares fit to the data has not been deemed appropriate, given the uncertainty of the measurements. The fits are, however, not

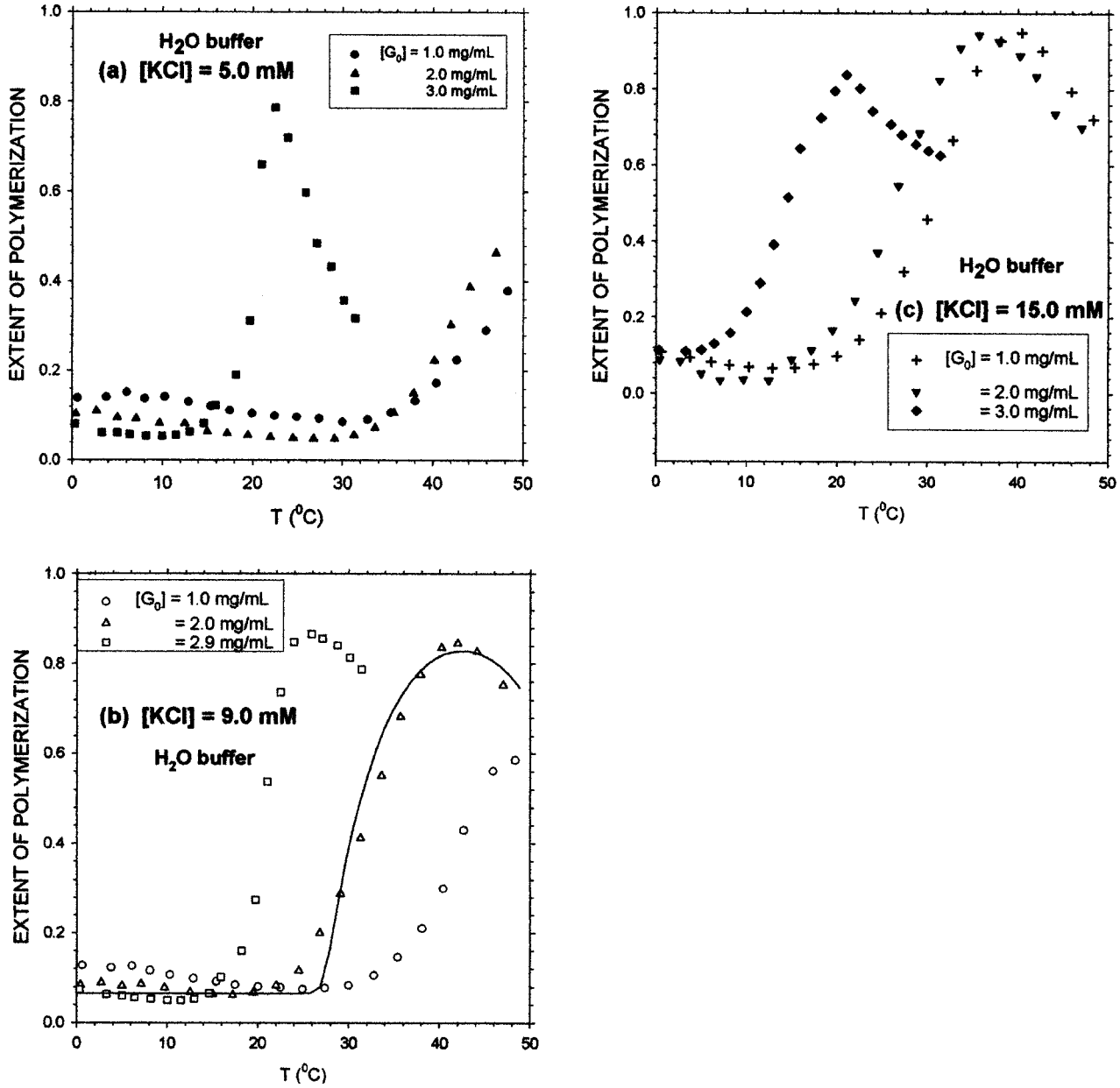

FIG. 3. Extent of polymerization Φ as a function of temperature for rabbit muscle actin in H_2O buffers at fixed [KCl]=(a) 5.0 mM, (b) 9.0 mM, and (c) 15.0 mM, for $[G_0]=1.00$ mg/ml, 2.00 mg/ml, and 2.93 mg/ml in each case. The line is the fit of the theory to the data (see text).

unique. A range of free energy parameters describes the data for a given sample equally well. Nonetheless, the signs of the parameters are uniquely determined, and certain ratios of parameters are constrained within narrow ranges, as described below in detail for the D_2O buffer systems. As independent experimental measurements of these parameters become available, this analysis can be refined.

The Flory–Huggins-type model describes the essential behavior of $\Phi(T)$, including the nonzero values at low temperatures, the increase in Φ with T, and the occurrence of a maximum in Φ at higher temperatures. The nonzero Φ at low temperature arises from the dimerization step in our model. As temperature increases, the dimerization slowly diminishes, as reflected (see Table IV below) in the negative fitted enthalpy and entropy changes for dimerization. The fits are especially insensitive to the dimerization parameters, and indeed the dimerization could be neglected in a first order model of the equilibrium polymerization.[48] Essentially, the only effect the dimerization parameters describe is the nonzero Φ at low temperatures.

The onset of the trimer/propagation step leads to an increase of Φ with T, which requires both the enthalpy and entropy changes for chain propagation to be positive,[48] as found for the fitted parameters previously reported.[20] An interestingresult of our analysis is that the signs of the enthalpy and entropy for the activation step in Eq. (1), are also positive, which means that the activation process also occurs substantially only above a characteristic temperature separate from T_p. The proximity of the onset of propagation (at which Φ increases) to the onset of activation (which reduces Φ by increasing the concentration of activated monomers) leads to the maximum in Φ.[20] Specifically, it is necessary for

TABLE I. Extent of polymerization of rabbit muscle actin in the H_2O buffer as a function of initial G-actin concentration, salt concentration, and temperature, T.

2.93 mg/ml actin				2.00 mg/ml actin				1.00 mg/ml actin			
T (°C)	4.8 mM KCl	9.0 mM KCl	14.3 mM KCl	T (°C)	5.0 mM KCl	9.0 mM KCl	15.0 mM KCl	T (°C)	5.0 mM KCl	9.0 mM KCl	15.0 mM KCl
0.3	0.080	0.074	0.11	0.4	0.10	0.085	0.088	0.6	0.14	0.13	0.11
3.3	0.061	0.064	0.11	2.7	0.11	0.090	0.084	3.8	0.14	0.12	0.09
5.0	0.062	0.060	0.11	5.0	0.095	0.082	0.051	6.1	0.15	0.13	0.082
6.4	0.058	0.056	0.13	7.1	0.093	0.087	0.034	8.1	0.14	0.12	0.073
8.2	0.054	0.053	0.16	9.7	0.083	0.079	0.036	10.3	0.14	0.11	0.069
10.0	0.054	0.050	0.21	12.5	0.081	0.068	0.033	12.9	0.13	0.099	0.065
11.5	0.056	0.050	0.29	15.0	0.064	0.064	0.088	15.4	0.12	0.092	0.067
13.0	0.063	0.053	0.39	17.2	0.060	0.063	0.11	17.5	0.11	0.085	0.077
14.6	0.082	0.066	0.52	19.5	0.056	0.068	0.17	20.0	0.10	0.081	0.098
15.9	0.12	0.10	0.64	22.0	0.052	0.083	0.25	22.5	0.10	0.079	0.14
18.2	0.19	0.16	0.73	24.5	0.049	0.12	0.37	24.9	0.097	0.075	0.21
19.7	0.31	0.27	0.80	26.8	0.048	0.20	0.55	27.4	0.093	0.078	0.32
21.0	0.66	0.54	0.84	29.1	0.048	0.29	0.69	30.0	0.085	0.084	0.46
22.5	0.79	0.74	0.80	31.3	0.055	0.41	0.83	32.8	0.091	0.11	0.67
23.9	0.72	0.85	0.74	33.6	0.072	0.55	0.91	35.4	0.11	0.15	0.85
25.9	0.60	0.87	0.71	35.7	0.11	0.68	0.94	38.1	0.13	0.21	0.93
27.1	0.48	0.86	0.68	37.9	0.15	0.78	0.93	40.4	0.17	0.30	0.95
28.7	0.43	0.84	0.66	40.2	0.22	0.84	0.89	42.7	0.22	0.43	0.90
30.1	0.36	0.81	0.64	42.0	0.30	0.85	0.84	45.9	0.29	0.56	0.79
31.4	0.32	0.79	0.63	44.1	0.39	0.83	0.74	48.3	0.38	0.59	0.72
				47.0	0.46	0.75	0.70				

$|\Delta H_{\text{actv}}| > \Delta H_{\text{prop}}|$ for the maximum to exist. In other words, this *coupling* between the activation and propagation processes is responsible for this effect. The dimerization has no effect on this feature, which would be seen in a model with only activation and propagation, subject to the conditions specified.

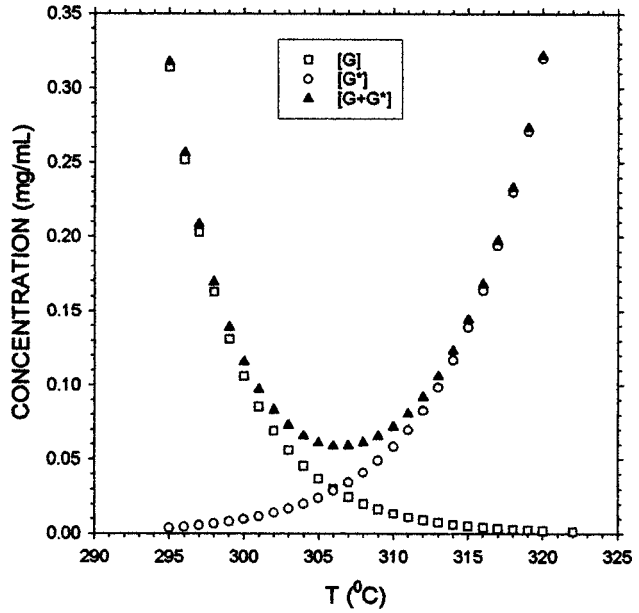

FIG. 4. Concentrations of free monomer, $[G]$, activated monomer, $[G^*]$, and their sum, as functions of temperature, for $[G_0]=2.93$ mg/ml and [KCl]=15 mM, in D_2O buffer. These concentrations are obtained from the fitted parameters in Table IV using the equations: $[1-\Phi(T)][G_0]=[G]+[G^*]$; $[G^*]=[G]\exp(-\Delta H_{\text{actv}}+T\Delta S_{\text{actv}})/RT\}$.

B. Extent of polymerization measurements in the D_2O buffer

Measurements have also been made for the extent of polymerization as a function of temperature in D_2O buffer A at the same actin and KCl concentrations levels as for the H_2O buffer measurements. The data are depicted in Figs. 5 and 6 and are presented in Table II.

1. General observations for D_2O buffers

The overall behavior of $\Phi(T)$ is similar to that in the H_2O buffer: The value of Φ is nonzero at low temperatures, grows with T over a broad range, achieves a maximum, and then decreases. As for H_2O buffer systems, T_p decreases as [KCl] is increased for $[G_0]$ fixed (see Fig. 5). However, below we describe the differences in the polymerization of actin between D_2O and H_2O buffers:

(1) Figures 6 and 7 and Table III indicate that for fixed [KCl] in the D_2O buffer, the shift in T_p is *not monotonic* in $[G]_0$: At 9.0 mM and 15.0 mM KCl, T_p for 2 mg/ml actin is *higher* than is the T_p for either 1 mg/ml or 3 mg/ml. For 5.0 mM KCl, the shifts in T_p with $[G]_0$ are within the scatter of our data. This behavior contrasts with that for the H_2O buffer, where the shift in T_p with actin concentration is monotonic (Fig. 3). Such a maximum has also been reported in a sol–gel transition line.[49]

(2) Table III exhibits the difference $[T_p(D_2O)-T_p(H_2O)]$ (°C) between the polymerization temperature in deuterated and hydrogenated buffers, for various [KCl] (mM) and $[G_0]$ (mg/ml). At high $[G_0]$ and high [KCl], we find $[T_p(D_2O)-T_p(H_2O)]>0$, while at low $[G_0]$ and low [KCl], the shift changes sign, $[T_p(D_2O)$

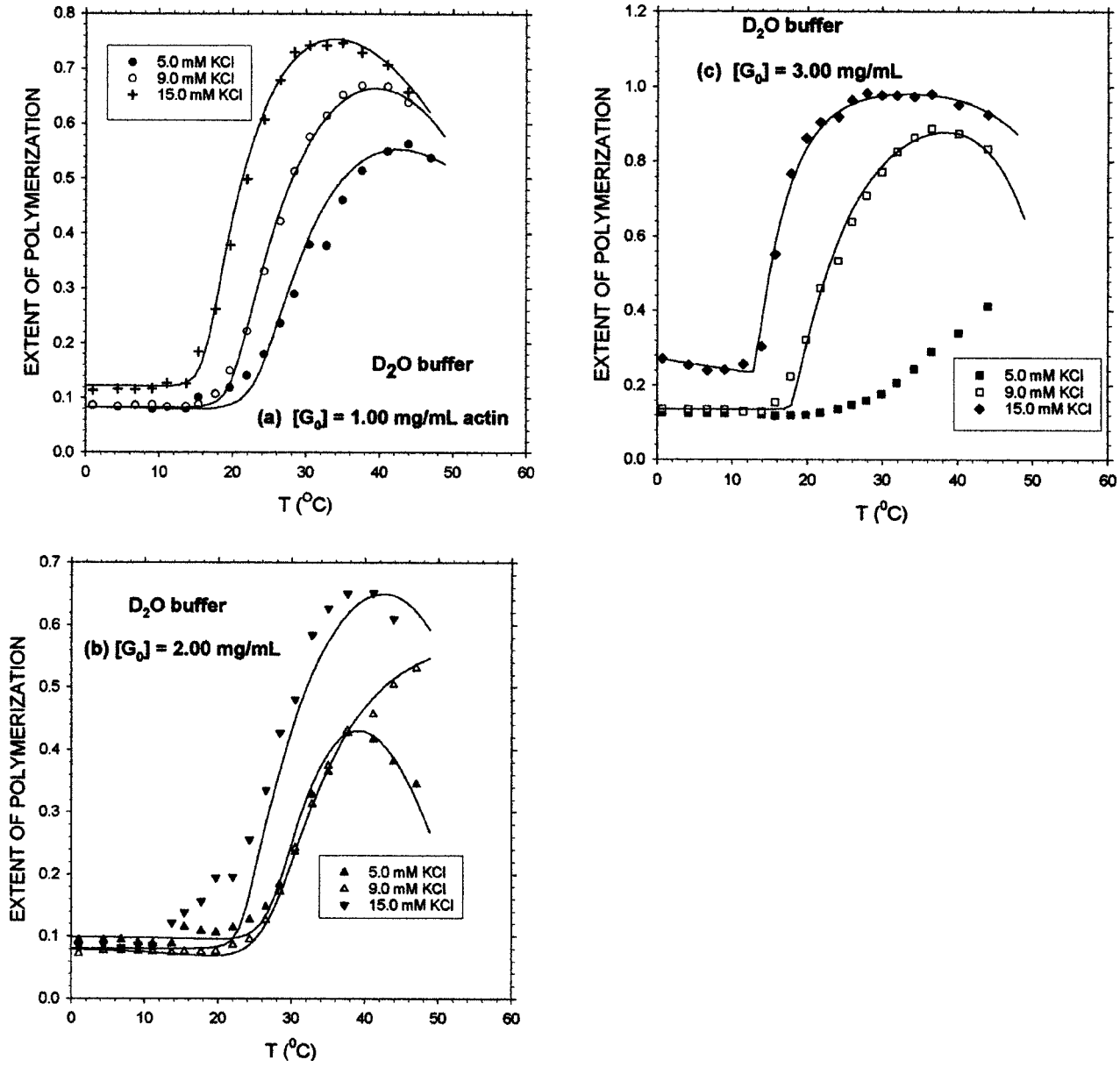

FIG. 5. Extent of polymerization Φ as a function of temperature for rabbit muscle actin in D_2O buffers for $[G_0]$=(a) 1.00 mg/ml, (b) 2.00 mg/ml, and (c) 2.93 mg/ml, for [KCl]=5.0 mM, 9.0 mM, and 15.0 mM in each case. The lines are the fits of the theory to the data (see text).

$-T_p(H_2O)]<0$. These values of T_p, taken as the points of inflection of $\Phi(T)$, are uncertain by about ± 2 °C, but the trends are clear.

2. Theoretical fits for D_2O buffers

Table IV displays the fitted parameters for the D_2O buffer, and Figs. 5 and 6 include both experimental data and theoretical calculations. The procedure for fitting to the $\Phi(T)$ data for the D_2O buffer is now described. We begin by fitting the unknowns in Eq. (24) to the low temperature tails of $\Phi(T)$, a procedure that determines $\Delta H_{\rm dim}+2\Delta H_{\rm actv}$ and $\Delta S_{\rm dim}+2\Delta S_{\rm actv}$. Although a range of values for these two quantities reproduces the experimental low temperature portion of $\Phi(T)$ equally well, the remaining four parameters are quite insensitive to this choice. Thus, a single value is chosen for $\Delta H_{\rm dim}+2\Delta H_{\rm actv}$ and $\Delta S_{\rm dim}+2\Delta S_{\rm actv}$, and then the remaining four parameters are fitted to the higher temperature parts of $\Phi(T)$. Finally, $\Delta H_{\rm init}$ and $\Delta S_{\rm init}$ are selected to locate the position and height of the maximum in the experimental $\Phi(T)$.

While the fits of the four parameters to experiment are not unique, certain ratios of the parameters are found to lie within a fairly narrow range that, of course, varies with the sample. The ratio $\Delta H_{\rm actv}/\Delta S_{\rm actv}$ obtained from good quality fits remains constant to within at most $\pm 5\%$ for all samples. On the other hand, the ratio $\Delta H_{\rm prop}/\Delta S_{\rm prop}$ for each of the samples is determined only to within the larger range of $\pm(10$–$20)\%$. The parameters for the activation and propagation steps are also inter-related. For example, fits for the sample with $[G_0]=1$ mg/ml and [KCl]=15 mM yield $\Delta H_{\rm prop}$ within a range of $\pm 20\%$ for a given $\Delta H_{\rm actv}$.

Given an uncertainty of $\pm 10\%$ between samples in the experimental data for (T), the theory explains the main features of the temperature variation of $\Phi(T)$ quite well. The

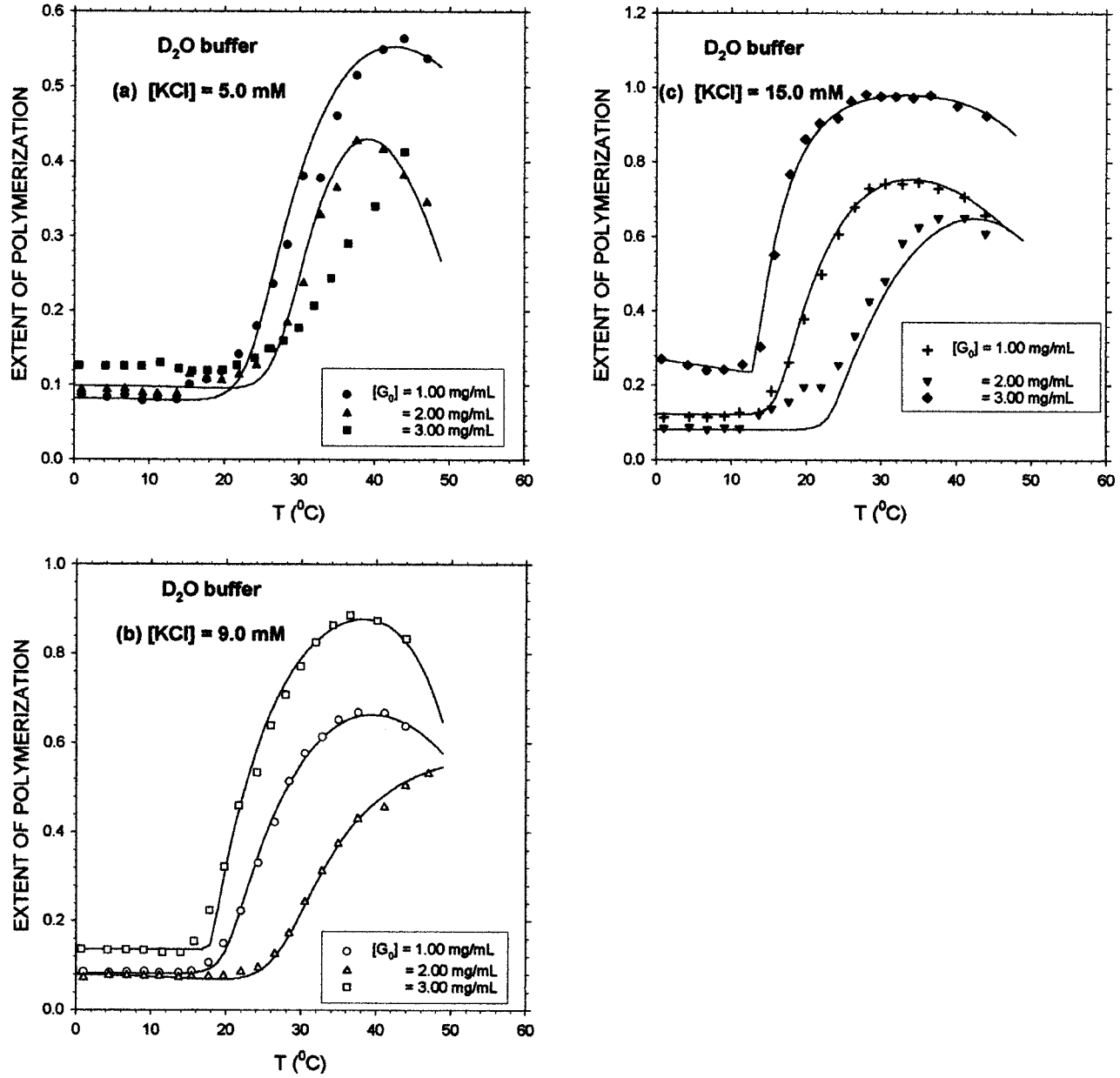

FIG. 6. Extent of polymerization Φ as a function of temperature for rabbit muscle actin in the D_2O buffer for [KCl]=(a) 5.0 mM (b) 9.0 mM, and (c) 15.0 mM, for $[G_0]=1.00$ mg/ml, 2.00 mg/ml, and 2.93 mg/ml in each case. The lines are the fits of the theory to the data (see text).

description of the low temperature tail and the unusual high temperature maximum require the use of a mechanism for actin polymerization with at least the three basic steps of actin activation, dimerization, and propagation (or their equivalents). Ratios of free energy parameters are constrained fairly narrowly, but individual parameters have larger percentage ranges of acceptable values. Other experimental observables (e.g., kinetic data for the same samples as a function of temperature) would be useful to constrain these parameters further.

V. CONCLUSIONS

We have performed experiments on rabbit muscle actin in H_2O buffers at relatively high actin concentrations and relatively low KCl concentrations, in the presence of Ca^{2+} and ATP. The extent of polymerization as a function of temperature exhibits a maximum, indicating the onset of a net depolymerization at high temperatures. For H_2O buffers, the polymerization temperature, T_p, decreases as either initial actin concentration, $[G_0]$, or [KCl] increases.

Analogous experiments in D_2O buffers display the same qualitative features, except that the shift of T_p with actin concentration at constant salt concentration is not monotonic. We do not understand this finding, nor is it evident how this effect can result from the theoretical model. Also, at low actin concentrations, $[G_0]=1.0$ mg/ml, we find that $T_p(D_2O)>T_p(H_2O)$, so that the polymerization of actin is greater in D_2O than in H_2O buffers at a given T. In contrast, at higher salt and actin concentrations, the situation reverses to $T_p(H_2O)>T_p(D_2O)$, i.e., higher polymerization occurs in H_2O buffer at a given T. Prior measurements on polymerizing proteins (for example, flagellin,[50] tobacco mosaic virus,[51]

TABLE II. Extent of polymerization of rabbit muscle actin in the D_2O buffer as a function of initial G-actin concentration, salt concentration, and temperature, *T*.

3.00 mg/ml actin				2.00 mg/ml actin				1.00 mg/ml actin			
T (°C)	5.00 mM KCl	9.00 mM KCl	15.00 mM KCl	*T* (°C)	5.00 mM KCl	9.00 mM KCl	15.00 mM KCl	*T* (°C)	5.00 mM KCl	9.00 mM KCl	15.00 mM KCl
0.7	0.13	0.14	0.27	1.0	0.094	0.072	0.081	1.0	0.087	0.086	0.11
4.2	0.13	0.13	0.25	4.4	0.094	0.077	0.085	4.4	0.084	0.084	0.12
6.7	0.13	0.14	0.24	6.8	0.095	0.077	0.088	6.8	0.087	0.086	0.11
9.0	0.13	0.14	0.24	9.1	0.090	0.076	0.082	9.1	0.079	0.087	0.12
11.5	0.13	0.13	0.26	11.1	0.088	0.076	0.086	11.1	0.083	0.084	0.13
13.9	0.12	0.13	0.30	13.7	0.088	0.073	0.086	13.7	0.081	0.084	0.13
15.7	0.12	0.15	0.55	15.4	0.11	0.076	0.12	15.4	0.10	0.088	0.18
17.8	0.12	0.22	0.77	17.7	0.11	0.075	0.14	17.7	0.11	0.11	0.26
19.8	0.12	0.32	0.86	19.7	0.11	0.076	0.16	19.7	0.12	0.15	0.38
21.7	0.13	0.46	0.91	22.0	0.11	0.086	0.20	22.0	0.14	0.22	0.50
24.1	0.14	0.53	0.92	24.3	0.13	0.096	0.20	24.3	0.18	0.33	0.61
25.9	0.15	0.64	0.96	26.5	0.15	0.13	0.26	26.5	0.24	0.42	0.68
27.9	0.16	0.71	0.98	28.4	0.18	0.17	0.34	28.4	0.29	0.51	0.73
29.9	0.18	0.77	0.98	30.5	0.24	0.24	0.43	30.5	0.38	0.58	0.74
31.9	0.21	0.83	0.98	32.8	0.33	0.31	0.48	32.8	0.38	0.61	0.74
34.2	0.24	0.86	0.97	35.0	0.36	0.37	0.58	35.0	0.46	0.65	0.75
36.5	0.29	0.89	0.98	37.6	0.43	0.43	0.63	37.6	0.52	0.67	0.73
40.1	0.34	0.88	0.95	41.1	0.42	0.46	0.65	41.1	0.55	0.67	0.71
44.0	0.41	0.83	0.93	43.9	0.38	0.51	0.65	43.9	0.56	0.64	0.66
				47.0	0.35	0.53	0.61	47.0	0.69		

and tubulin[52]) indicate that a D_2O buffer promotes polymerization. The only prior study for actin (chicken muscle actin[53] at 0.3 mg/ml actin with 100 mM KCl and 2 mM $MgCl_2$) reports identical extents of polymerization for H_2O and D_2O buffers. Our experimental results demonstrate that the shift from H_2O to D_2O buffers is not a minor perturbation on protein behavior as is sometimes assumed. The competitive influences of hydrogen bonding, salt concentration, etc., on the differences between these buffers remain to be studied further.

The origin of the driving force for actin polymerization is the *increase* in entropy that results when the monomers come together to form polymers. The increase in entropy is thought to be due to the release of hydrogen bonds between the actin monomers and water and subsequent formation of hydrophobic associations between the monomers in the polymer. The deuteration of the water changes the interactions significantly and thus alter the energies and entropies of the steps of the polymerization. Deuterium bonds are known to be stronger than protonated hydrogen bonds,[54] so they would favor the depolymerization (i.e., G-actin). The extent of hydrophobic interactions changes with the formation of F-actin, due to the alterations in the local surface area exposed to

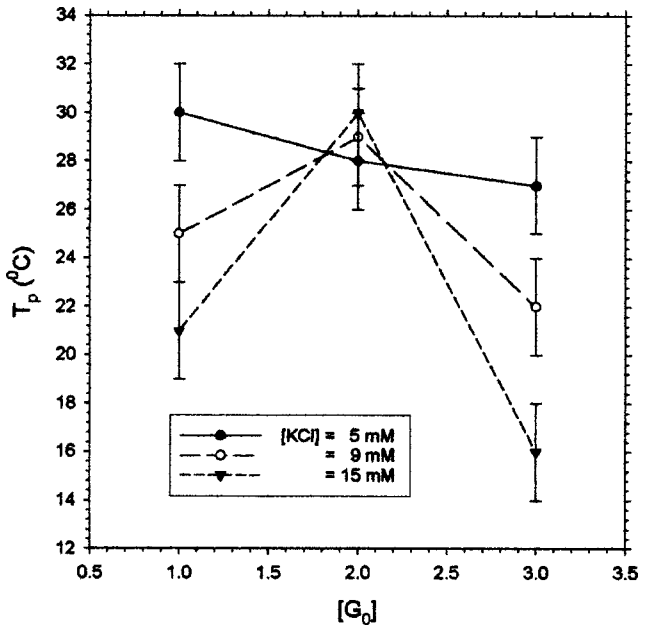

FIG. 7. Polymerization temperatures T_p in D_2O buffers, as a function of $[G_0]$ for fixed [KCl]. The error bars for T_p are estimated at ±2 °C, based on Fig. 1(c).

TABLE III. Experimental polymerization temperatures, T_p, for various samples with different concentrations of KCl and initial G-actin. T_p values were determined from the points of inflection of the extent of polymerization, Φ, as a function of *T*. The uncertainties in T_p are ±(2–3) °C. Some T_p values could not be determined because the $\Phi(T)$ did not extend to a sufficiently high *T*.

[KCl] (mM)	$[G_0]$ (mg/ml)	$T_p(H_2O)$ (°C)	$T_p(D_2O)$ (°C)	$T_p(D_2O) - T_p(H_2O)$
5.00	3.00	21		
9.00	3.00	20	22	2
15.00	3.00	13	16	3
5.00	2.00	39	28	−11
9.00	2.00	32	29	−3
15.00	2.00	28	30	2
5.00	1.00		30	
9.00	1.00	41	25	−16
15.00	1.00	31	21	−10

TABLE IV. Free energy parameters for the polymerization of actin in the D_2O buffer, as obtained from fits to theory.

Parameters [KCl] (mM)=	5		9			15		
$[G_0]$ (mg/ml)=	1	2	1	2	3	1	2	3
ΔH^0_{actv} (kJ/mol)	110	145	130	100	250	150	150	300
ΔS^0_{actv} (J/mol K)	356	468	417	328	798	494	472	980
ΔH^0_{dim} (kJ/mol)	−220	−290	−260	−200	−500	−300	−300	−613
ΔS^0_{dim} (J/mol K)	−606	−834	−728	−555	−1494	−888	−844	−1897
ΔH^0_{prop} (kJ/mol)	80	90	70	100	90	100	60	160
ΔS^0_{prop} (J/mol K)	410	434	379	469	441	486	337	692

solvent. Hydrophobic effects are thought to depend, in part, on the size of the hydrophobic species.[55,56] For large hydrophobes such as actin [the diameter of the actin monomer is about 5 nm (Ref. 25)], the hydrophobic interactions can lead to a net loss of hydrogen bonds in order to fit the hydrophobe into the water. Again, deuterium bonds are stronger than hydrogen bonds, so hydrophobic effects can be expected to be stronger in D_2O than in H_2O, and consequently the D_2O solvent would seem to promote polymerization, as is usually seen. In the case that the hydrophobic species has only repulsive interactions with the solvent, proximity to the liquid vapor phase transition has been argued to cause further ''drying'' at the surface of the hydrophobe and, thus, enhance hydrophobic interactions.[55,57] The boiling point of D_2O is 374.59 K,[58] compared to 373.15 K for H_2O, so the deuterated solvent is further from the boiling point. Here the proximity argument would predict reduced hydrophobic effects in D_2O, not the enhanced effects that we observe at low [KCl] and low $[G_0]$. This disagreement may be due to the fact that the interactions between the ''hydrophobe'' and the solvent are not purely repulsive. Indeed, the actin monomer is highly charged and has a surface that contains polar groups, and some charged and polar groups must form hydrogen bonds with the solvent. Apparently several competing factors conspire to produce the observed nonmonotonic dependence of T_p on $[G_0]$ in the D_2O buffers. The significance of this effect is that we must take care in use deuterated samples to infer physical characteristics of hydrogenated systems.

We successfully describe the thermodynamics of the polymerization of actin by a Flory–Huggins-type lattice model which includes the following essential steps: an activation reaction, a dimerization of two activated species that is enhanced at low temperatures, the formation of a trimer as the smallest propagating oligomer, and the propagation of trimers into higher polymers. Several other polymerization mechanisms with the same basic steps produce essentially identical results upon redefinition of the energy parameters of the model. An important result of our analysis is the proximity of the temperatures of onset for activation and propagation and the resulting coupling between these two steps. That coupling leads to the maximum in the extent of polymerization and may be related to other features of the polymerization of actin.

Actin polymerization is crucial to cell structure and movement and may be controlled by changes in thermodynamic parameters, as our experiments show by varying temperature and salt concentration.

ACKNOWLEDGMENTS

This work was supported by the National Institute of Arthritis and Musculoskeletal and Skin Diseases (AR45191) and the National Institutes of General Medicine (GM56678) of the NIH. We thank N. Blough for the use of his spectrometer, Michael Alessi for help with actin purification, and S. De for help with the calculations.

[1] D. J. DeRosier, Nature (London) **347**, 21 (1990).
[2] J. A. Theriot and T. J. Mitchison, Nature (London) **352**, 126 (1991); J. Lee, A. Ishihara, J. A. Theriot, and K. Jacobsen, *ibid.* **362**, 167 (1993); J. A. Spudich, *ibid.* **372**, 515 (1994).
[3] L. A. Amos and W. B. Amos, *Molecules of the Cytoskeleton* (The Guilford Press, New York, 1991).
[4] T. D. Pollard and J. A. Cooper, Annu. Rev. Biochem. **55**, 987 (1986).
[5] M. Irving and Y. E. Goldman, Nature (London) **398**, 463 (1999).
[6] D. Pantaloni, C. L. Clainche, and M.-F. Carlier, Science **292**, 1502 (2001).
[7] K. Svoboda, C. F. Schmidt, B. J. Schnapp, and S. M. Block, Nature (London) **365**, 721 (1993).
[8] T. P. Stossel, Sci. Am. **271**, 54 (1994); D. A. Lauffenburger and A. L. Horwitz, Cell **84**, 359 (1996).
[9] P. A. Janmey, Annu. Rev. Physiol. **56**, 169 (1994); J. Condelis, Annu. Rev. Cell Biol. **9**, 411 (1993).
[10] F. Oosawa and S. Asakura, *Thermodynamics of the Polymerization of Protein* (Academic, New York, 1975).
[11] R. Ivkov, J. G. Forbes, and S. C. Greer, J. Chem. Phys. **108**, 5599 (1998).
[12] M. Szwarc, *Carbanions, Living Polymers, and Electron Transfer Processes* (Wiley, New York, 1968).
[13] J. C. Wheeler, S. J. Kennedy, and P. Pfeuty, Phys. Rev. Lett. **45**, 1748 (1980).
[14] S. C. Greer, Annu. Rev. Phys. Chem. **53**, 173 (2002).
[15] J. Dudowicz, K. F. Freed, and J. F. Douglas, J. Chem. Phys. **113**, 434 (2000); **112**, 1002 (2000).
[16] J. Dudowicz, K. F. Freed, and J. F. Douglas, J. Chem. Phys. **111**, 7116 (1999).
[17] S. S. Das, A. P. Andrews, and S. C. Greer, J. Chem. Phys. **102**, 2951 (1995).
[18] S.-K. Ma, *Modern Theory of Critical Phenomena* (Benjamin/Cummings, Reading, 1976).
[19] J. Dudowicz, K. F. Freed, and J. F. Douglas (unpublished).
[20] P. S. Niranjan, J. G. Forbes, S. C. Greer, J. Dudowicz, K. F. Freed, and J. F. Douglas, J. Chem. Phys. **114**, 10573 (2001).
[21] The accepted SI unit of concentration (mol/l) is represented in this paper by its historically used symbol (M).
[22] C. S. Heacock and J. R. Bamburgh, Anal. Biochem. **135**, 22 (1983).
[23] M. Kasai, Biochim. Biophys. Acta **180**, 399 (1969); R. R. Swezey and G. N. Somero, Biochemistry **21**, 4496 (1982).
[24] H. J. Kinosian, L. A. Selden, J. E. Estes, and L. C. Gershman, Biochim. Biophys. Acta **1077**, 151 (1991).
[25] P. Sheterline, J. Clayton, and J. C. Sparrow, *Actin*, 4th ed. (Oxford University Press, Oxford, 1998).
[26] P. J. Flory, *Principles of Polymer Chemistry* (Cornell University Press, Ithaca, 1953).
[27] L. A. Selden, H. J. Kinosian, J. E. Estes, and L. C. Gershman, Biochemistry **39**, 64 (2000).

[28] K. C. Holmes, D. Popp, W. Gebhard, and W. Kabsch, Nature (London) **347**, 44 (1990).
[29] J. A. Cooper, J. E. Loren Buhle, S. B. Walker, T. Y. Tsong, and T. D. Pollard, Biochemistry **22**, 2193 (1983).
[30] F. Oosawa and M. Kasai, J. Mol. Biol. **4**, 10 (1962); A. Wegner and J. Engel, Biophys. Chem. **3**, 215 (1975).
[31] M. G. Bawendi and K. F. Freed, J. Chem. Phys. **86**, 3720 (1987).
[32] J. A. Cooper and T. D. Pollard, in *Methods in Enzymology: Structural and Contractile Proteins, Part B, The Contractile Apparatus and the Cytoskeleton*, edited by D. W. Frederiksen and L. D. Cunningham (Academic, New York, 1982), Vol. 85, p. 182.
[33] J. A. Cooper, S. B. Walker, and T. D. Pollard, J. Muscle Res. Cell Motil. **4**, 253 (1983).
[34] P. B. Yim, D. T. Jacobs, N. D. Peters, J. G. Forbes, M. L. Alessi, and S. C. Greer (unpublished).
[35] P. S. Niranjan, J. G. Forbes, and S. C. Greer, Biomacromolecules **1**, 506 (2000).
[36] Certain commercial materials and equipment are identified in this article in order to specify adequately the experimental procedure. In no case does such identification imply recommendation by the NIST nor does it imply that the material or equipment identified is necessarily the best available for this purpose.
[37] J. D. Pardee and J. A. Spudich, in *Methods in Enzymology: Structural and Contractile Proteins, Part B, The Contractile Apparatus and the Cytoskeleton*, edited by D. W. Frederiksen and L. W. Cunningham (Academic, New York, 1982), Vol. 85, p. 164.
[38] T. Kouyama and K. Mihashi, Eur. J. Biochem. **114**, 33 (1981).
[39] S. Maclean-Fletcher and T. D. Pollard, Biochem. Biophys. Res. Commun. **96**, 18 (1980); T. W. Houk and K. Ue, Anal. Biochem. **62**, 66 (1974).
[40] P. S. Niranjan, Ph.D. thesis, University of Maryland, College Park, 2000.
[41] F. S. Dainton and K. J. Ivin, Q. Rev., Chem. Soc. **12**, 61 (1958).
[42] R. F. Bacon and R. Fanelli, J. Am. Chem. Soc. **65**, 639 (1943).
[43] P. Ballone and R. Jones, J. Chem. Phys. (to be published).
[44] T. C. Tsao, Biochim. Biophys. Acta **11**, 227 (1953); D. W. Goddette, E. C. Uberbacher, G. J. Bunick, and C. Frieden, J. Biol. Chem. **261**, 2605 (1986).
[45] C. T. Zimmerle and C. Frieden, Biochemistry **25**, 6432 (1986).
[46] Y. Sasaki, F. Tsunomori, T. Yamashita, K. Horie, H. Ushiki, R. Ishikawa, and K. Kohama, J. Biochem. (Tokyo) **116**, 236 (1994).
[47] M. L. McGlashan, *Chemical Thermodynamics* (Academic, New York, 1979); G. Weber, J. Phys. Chem. **99**, 1052 (1995); **99**, 13051 (1995).
[48] H. Sawada, *Thermodynamics of Polymerization* (Dekker, New York, 1976).
[49] F. Tanaka, Macromolecules **23**, 3790 (1990).
[50] Y. Uratani, J. Biochem. (Tokyo) **75**, 1143 (1974).
[51] M. Thanaa, M. Khalil, and M. A. Lauffer, Biochemistry **6**, 2474 (1967).
[52] D. Panda, G. Chakrabarti, J. Hudson, K. Pigg, H. P. Miller, L. Wilson, and R. H. Himes, Biochemistry **39**, 5075 (2000); G. Chakrabarti, S. Kim, J. Mohan, L. Gupta, J. S. Barton, and R. H. Himes, *ibid.* **38**, 3067 (1999).
[53] H. Omori, M. Kuroda, H. Naora, H. Takeda, Y. Nio, H. Otani, and K. Tamura, Eur. J. Cell Biol. **74**, 273 (1997).
[54] A. Engdahl and B. Nelander, J. Chem. Phys. **86**, 1819 (1987).
[55] K. Lum, D. Chandler, and J. D. Weeks, J. Phys. Chem. B **103**, 4570 (1999).
[56] N. T. Southall, K. A. Dill, and A. D. J. Haymet, J. Phys. Chem. B **106**, 521 (2002).
[57] D. Chandler, Nature (London) **417**, 491 (2002).
[58] A. I. Shatenshtein, E. A. Yakovleva, E. A. Zvyagintseva, E. N. Varshavskii, M. Ya, E. J. Israelevich, and N. M. Dykhno, *Isotopic Water Analysis*, 2nd ed. (United States Atomic Energy Commission, Washington, D.C., 1960).